Supplemental Information

Tumor-Associated Macrophages Drive Spheroid Formation During Early Transcoelomic Metastasis of Ovarian Cancer

Mingzhu Yin et al

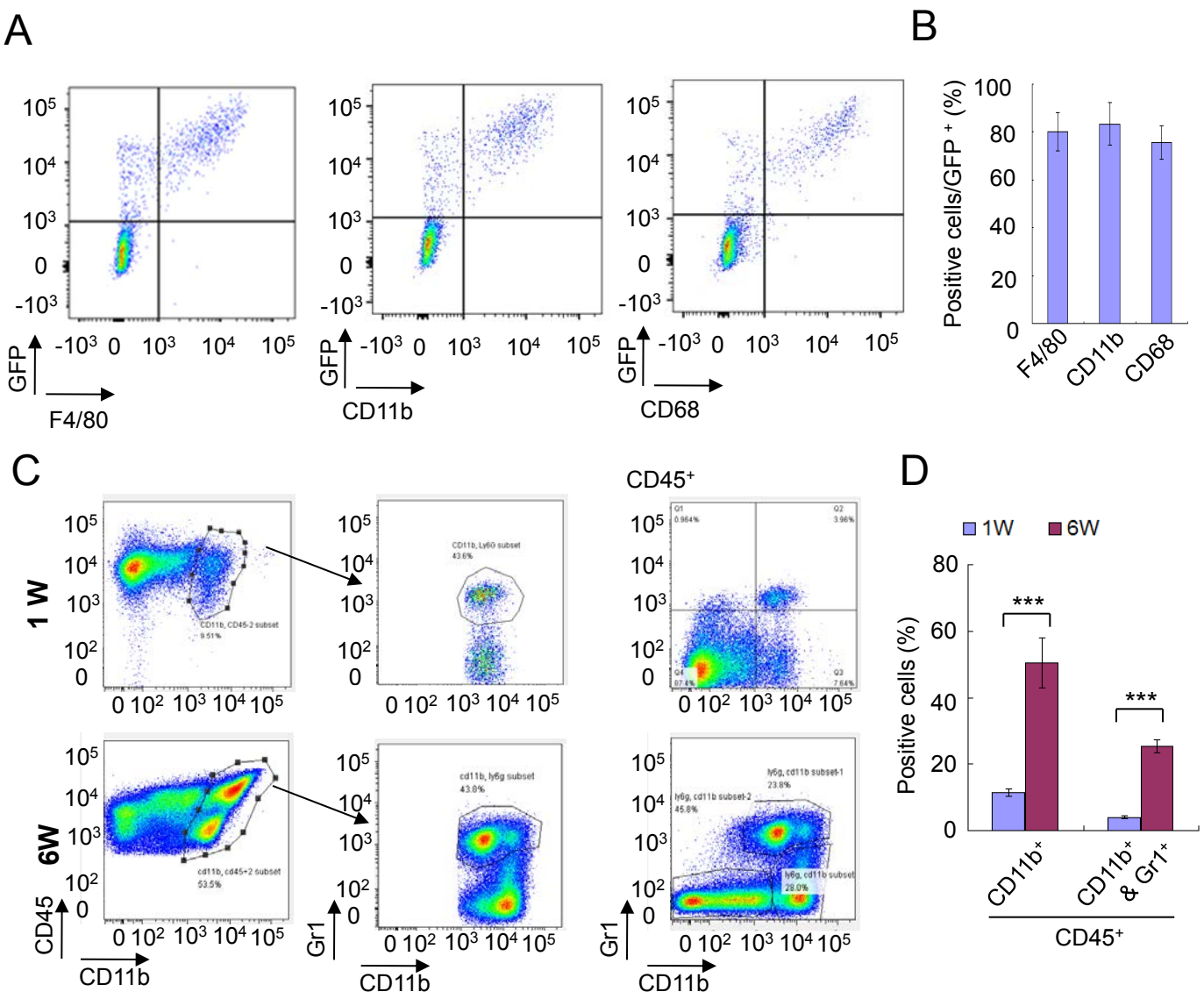

Supplemental Figure 1. Characterization of peritoneal macrophages. (**A-B**) GFP$^+$ cells infiltrated into peritoneal cavity were F4/80$^+$, CD11b$^+$ and CD68$^+$ macrophages. Total peritoneal cells were harvested at various time points (2 h, 2-8 weeks) and were stained with anti-F4/80, CD11b and CD68 followed by FACS analyses. Representative images in (**A**) are shown for samples at 8 weeks. % of F4/80$^+$, CD11b$^+$ and CD68$^+$ in the GFP$^+$ cell populations were quantified in (**B**), n=5. (**C-D**) CD11b$^+$ macrophages and CD11b$^+$Gr1$^+$ myeloid-derived suppressor cells in ascites at 1 and 6 weeks were analyzed by FACS (**C**). % of CD11b$^+$ and CD11b$^+$Gr$^+$ cells were quantified (**D**), n=5, ***, P<0.001; (two-sided student's t-test).

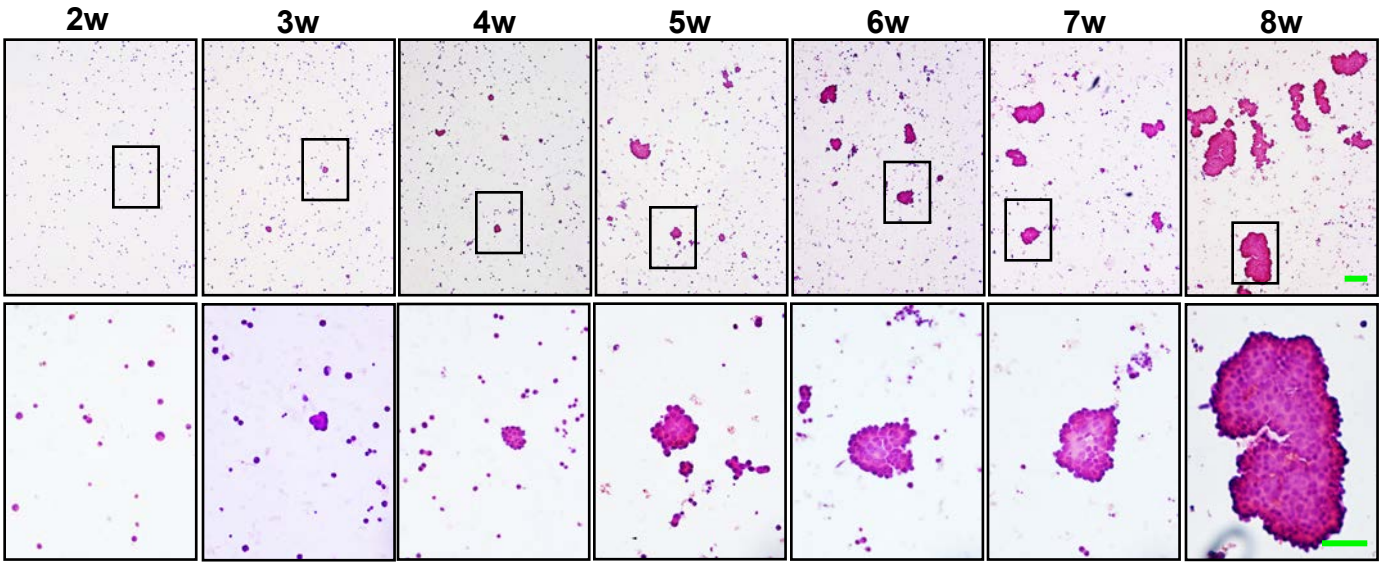

Supplemental Figure 2. Characterization of spheroids from mouse OC models. Spheroids from ascites were collected and examined by H&E staining. Representative images of n=5 mice for each time point are shown. Spheroids were detected at week 3 and rapidly increased from week 4-8. Scale bar, 10 μm.

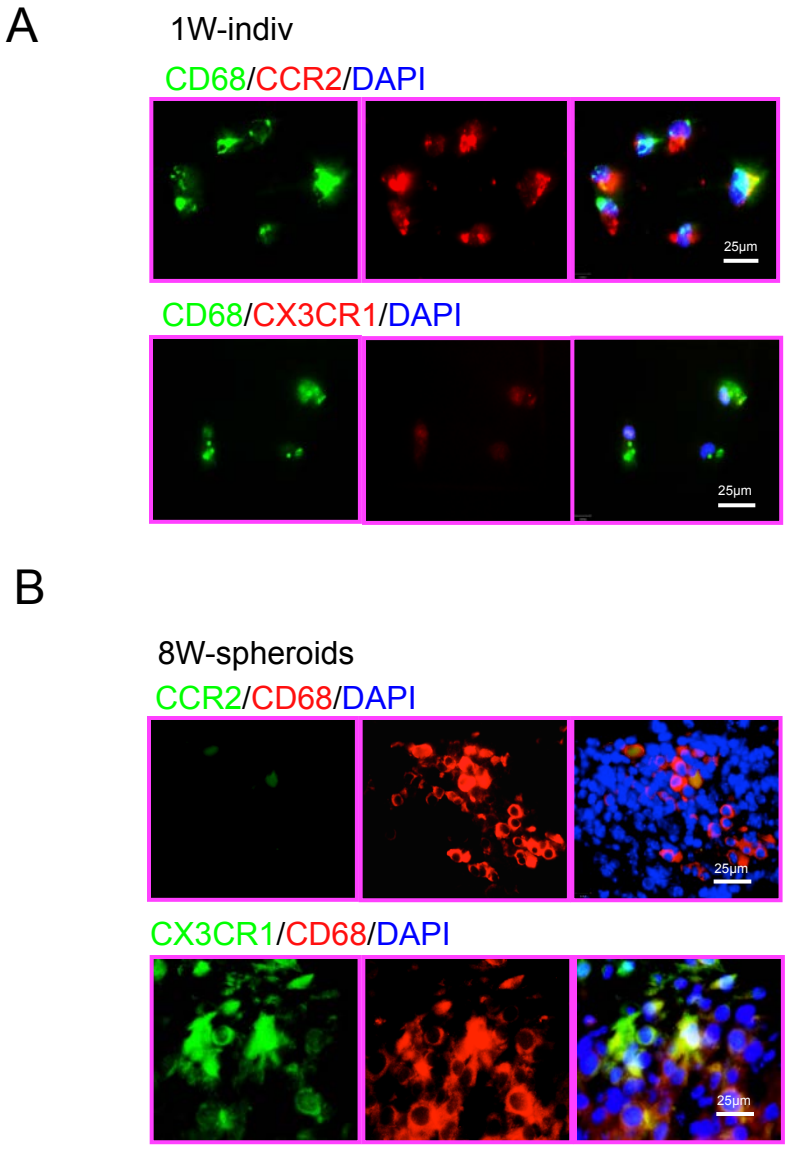

Supplemental Figure 3. CCR2 and CX3CR1 expression in individual cells and spheroids. (**A**) Immunofluorescent staining of CD68 together with CCR2 or CX3CR1 for week 1 individual cells. Scale bar, 25μm. n=5. (**B**) Immunofluorescent staining of CD68 together with CCR2 or CX3CR1 for week 8 spheroids. Scale bar, 25μm. n=5.

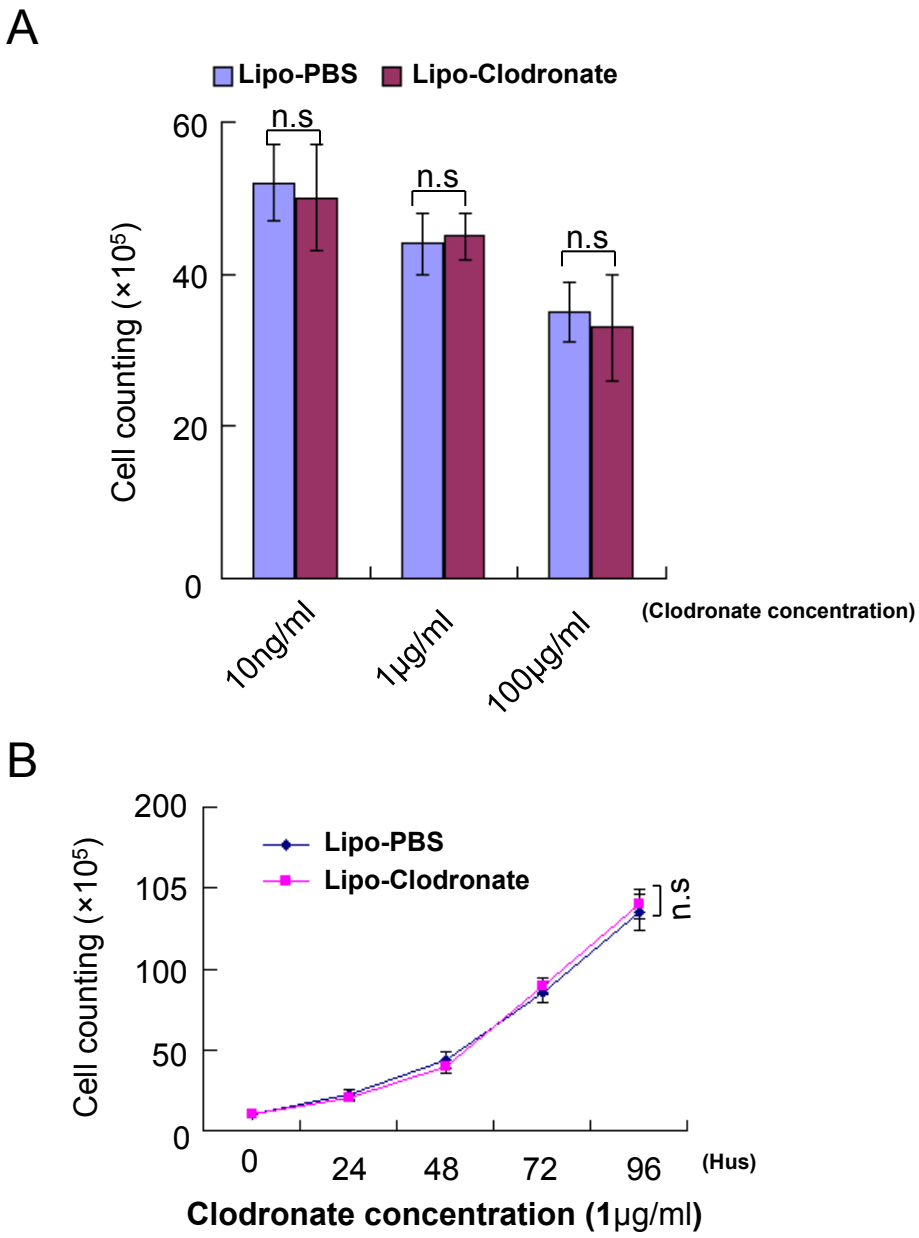

Supplemental Figure 4. Clodronate cannot inhibits tumor cell proliferation in vitro. (**A**) Cell counting of the cell proliferation between liposome-PBS and liposome-Clodronate groups in response to clodronate treatment for 24 h at different concentrations. Data are presented as Mean ± SEM. ns: non-significance. (n=4). (**B**) Cell counting of the cell proliferation between liposome-PBS and liposome-Clodronate groups in response to clodronate treatment for 1μg/ml at different time point. Data are presented as Mean ± SEM. ns: non-significance. (n=4) (two-sided student's t-test).

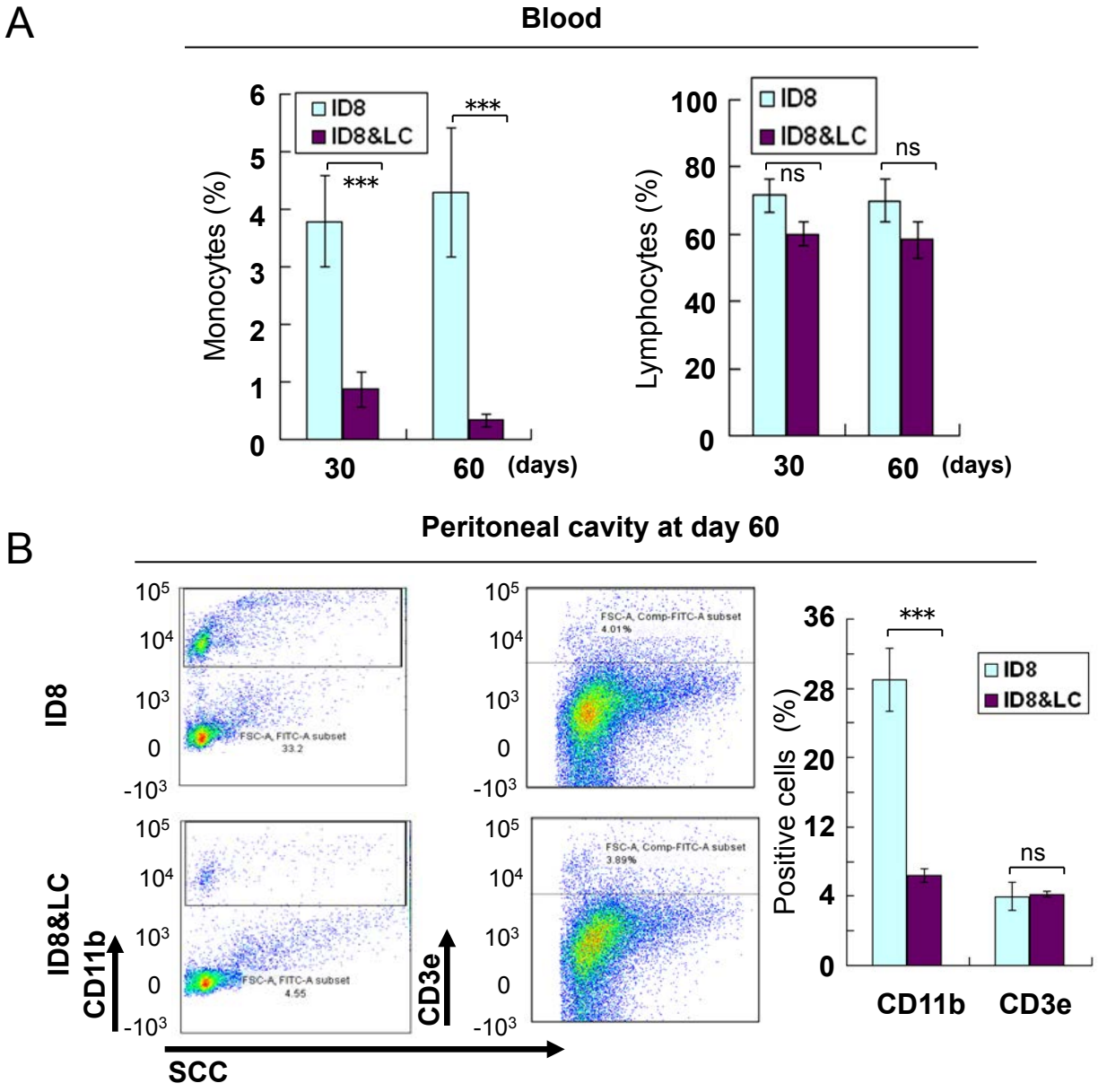

Supplemental Figure 5. Liposome clodronate eliminates macrophages in blood and peritoneal cavity. (**A**) Monocytes and lymphocytes in blood of control and LC-treated mice were analyzed by complete blood cell counting (CBC) at indicated time points (day 30 and day 60 post-tumor cell implantation). % of monocytes and % of lymphocytes were quantified, n=5, ***, $P<0.001$; ns: non-significance.
(**B**) $CD11b^+$ macrophages and $CD3e^+$ T cells in peritoneal cavity were analyzed by FACS. % of $CD11b^+$ macrophages and % of $CD3e^+$ T cells were quantified, n=5, ***, $P<0.001$; ns: non-significance. (two-sided student's t-test).

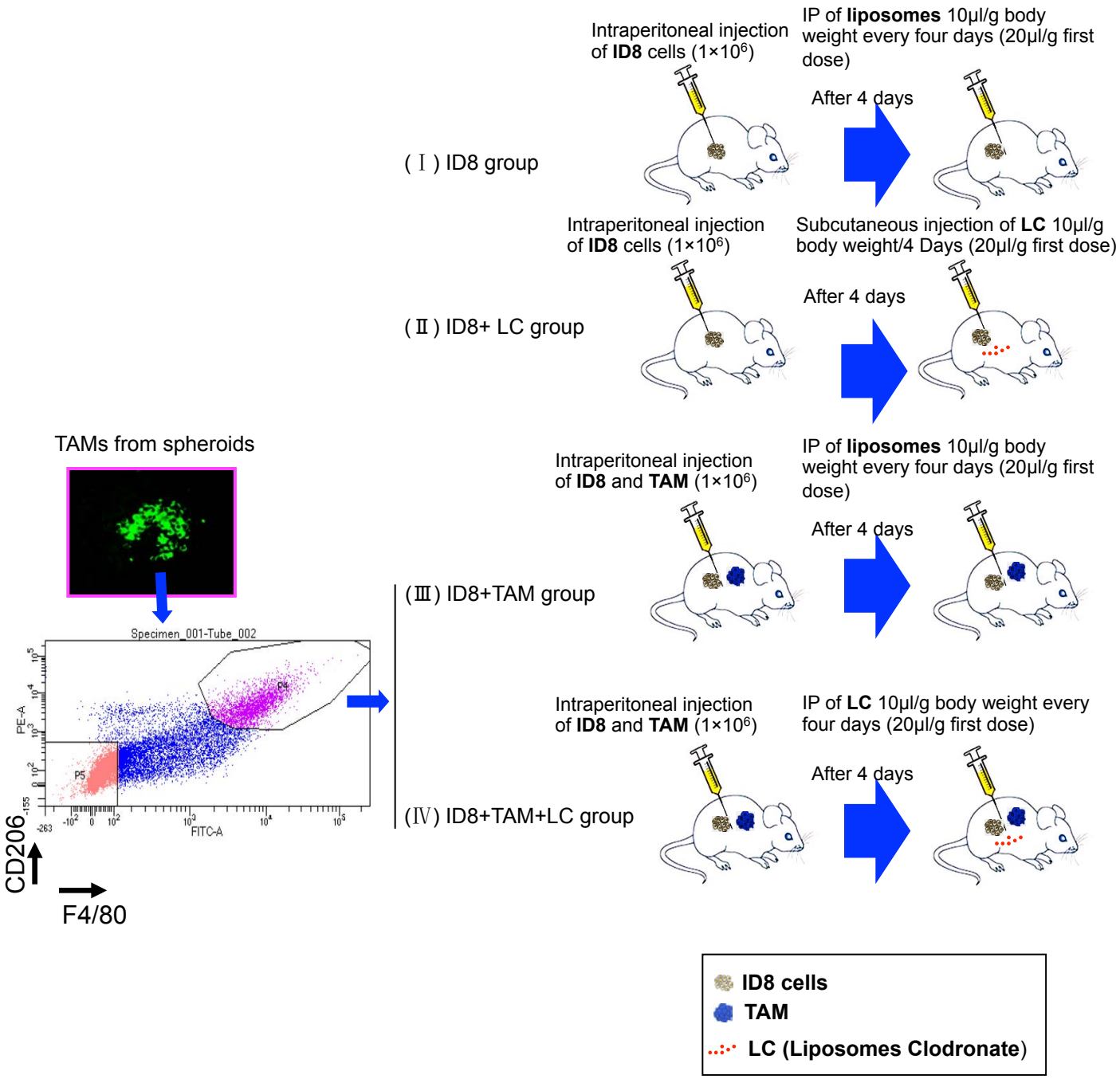

Supplemental Figure 6. Schematics for mouse groups.
ID8 cells (1×10^6) alone (ID8) or with liposome clodronate (ID8+LC) or with (1×10^6 of $4/80^+$ $CD206^+$ TAMs) isolated from spheroids of ovarian cancer-bearing donor mice (ID8+TAM) were injected into peritoneal cavity of new recipient mice. Recipient mice were treated with liposome or treated with liposome clodronate (ID8+TAM+LC).

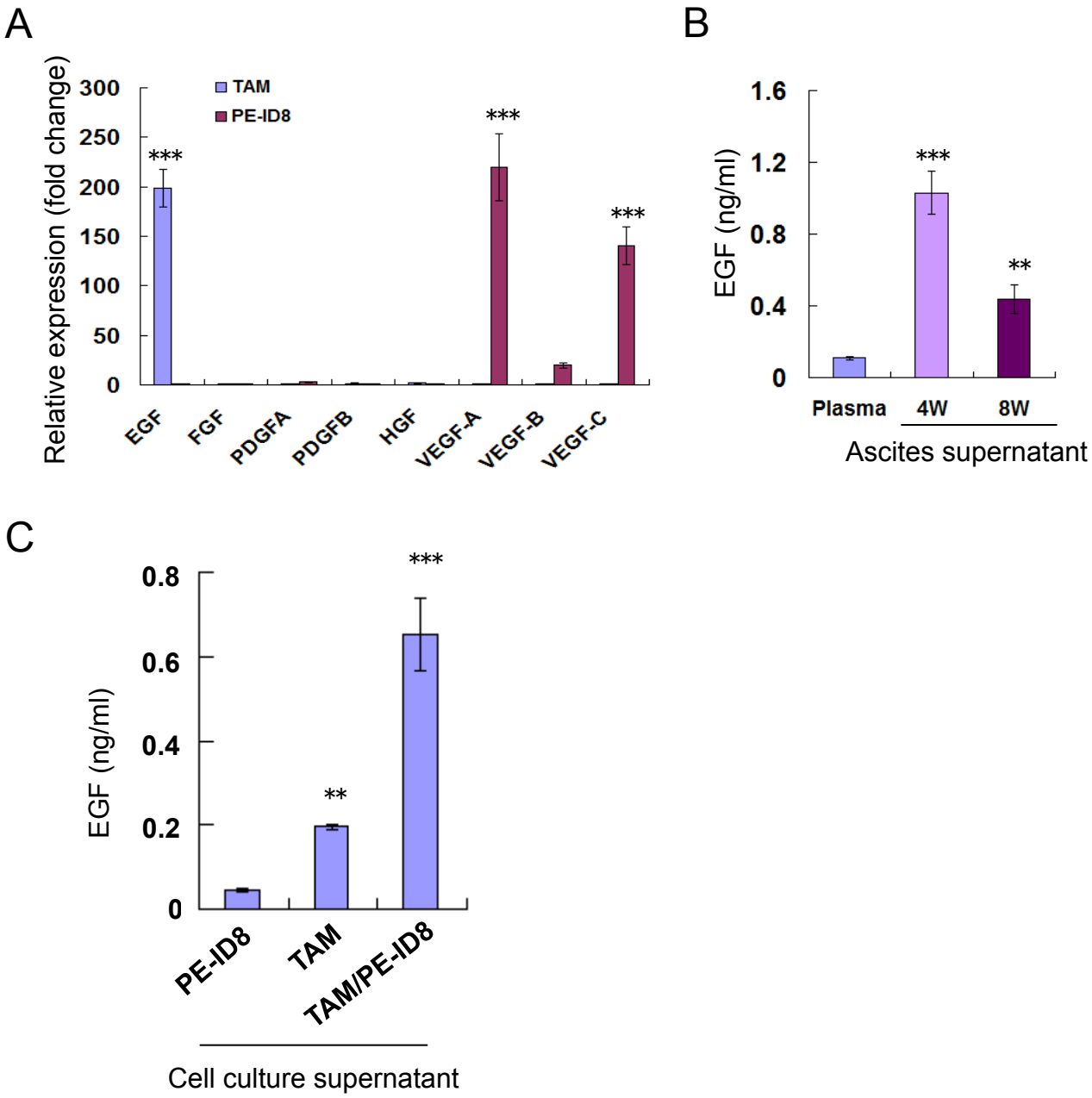

Supplemental Figure 7. EGF expression and secretion from TAM. (**A**) Gene expressions of EGF, FGF, PDGFs, HGF and VEGFs in TAMs and PE-ID8 were determined by qRT-PCR. (**B**) ELISA analysis of EGF protein expression in ascites at 4 and 8 weeks post-tumor injection. Plasma was used as a negative control. (**C**) ELISA analysis of EGF protein expression in supernatants of tumor cells, TAMs with or without co-culture of TAMs. Data are presented as means ± SEM, n=3; **, $P<0.01$; ***, $P<0.001$ (two-sided student's *t*-test).

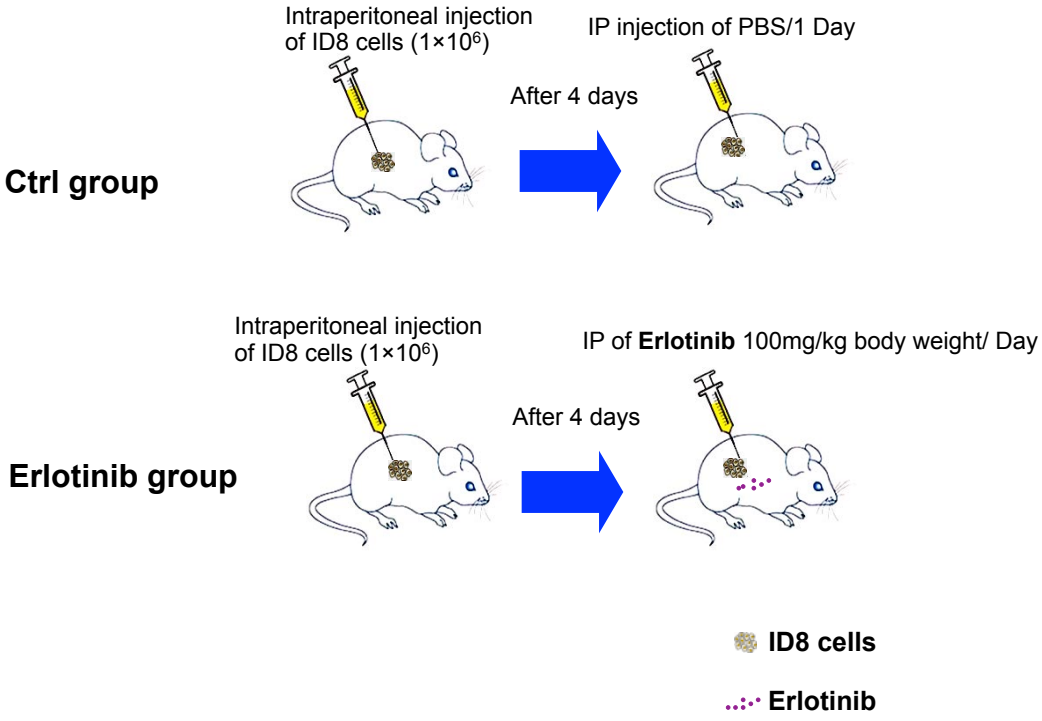

Supplemental Figure 8. Schematics for mouse groups. An orthotopic mouse model was established by injecting mouse ID8 OCs (1×10^6) intraperitoneally to C57BL/6 female recipient mice. Mice were then either treated with PBS (ID8 group) or treated with Erlotinib (Erlotinib group) from day 4 post-tumor cell implantation by IP injection at 100mg/kg body weight every one day.

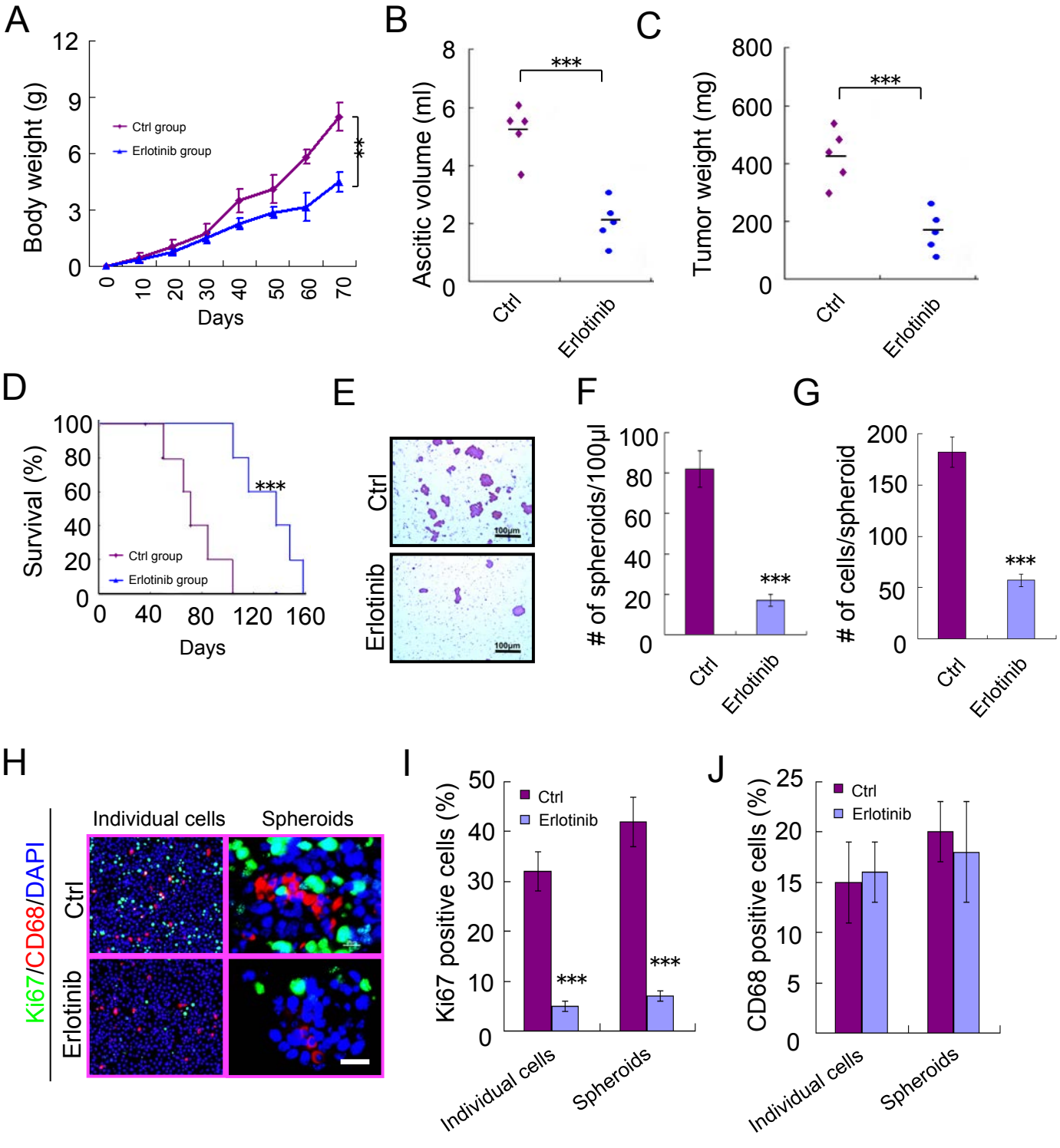
A
Body weight (g)
Ctrl group
Erlotinib group
**
Days
B
Ascitic volume (ml)
***
Ctrl
Erlotinib
C
Tumor weight (mg)
***
Ctrl
Erlotinib
D
Survival (%)
***
Ctrl group
Erlotinib group
Days
E
Ctrl
Erlotinib
100μm
F
# of spheroids/100μl
***
Ctrl
Erlotinib
G
# of cells/spheroid
***
Ctrl
Erlotinib
H
Individual cells
Spheroids
Ki67/CD68/DAPI
Ctrl
Erlotinib
I
Ki67 positive cells (%)
Ctrl
Erlotinib
***
***
Individual cells
Spheroids
J
CD68 positive cells (%)
Ctrl
Erlotinib
Individual cells
Spheroids

Supplemental Figure 9. EGFR inhibitor inhibits spheroid formation and tumor growth of ovarian cancer. An orthotopic mouse model was established by injecting mouse ID8 OCs (1×10^6) intraperitoneally to C57BL/6 female recipient mice. Mice were then either treated with PBS (Ctrl group) or treated with Erlotinib (Erlotinib group) from day 4 post-tumor cell implantation subcutaneous injection at 100mg/kg body weight every day. (**A**) Mouse body weights were measured at indicated time points (day 0-70). (**B,C**) Ascites volumes and net tumor weights were measured at day 70. All data are presented as means ± SEM, n=10, ***, P<0.001 (two-sided student's t-test). (**D**) Mouse modality was monitored and survival rates were quantified, n=12 mice per group. Kaplan-Meier analyses using the log-rank test was performed, ***, P<0.001.

(**E-G**) Effects of Erlotinib on spheroid formation. Spheroids from ascites were collected at week 8 and mounted on slides. Spheroids were examined by H&E staining (**E**), Scale bar, 100 μm. Total number (**F**) and size (**G**) of spheroids were quantified. Data are presented as means ± SEM, n=10, ***, P<0.001 (two-sided student's t-test). (**H-J**) Effects of Erlotinib on tumor cell proliferation. Individual cells and spheroids collected at week 8 were subjected to immunostaining with anti-Ki67, anti-CD68 and DAPI followed by confocal imaging. (**H**) Representative images showing $CD68^+$ macrophages are surrounded by $Ki67^+$ tumor cells in ID8 but not in ID8+Erlotinib group. Scale bar, 25 μm. $Ki67^+$ (**I**) and $CD68^+$ cells (**J**) in individual and spheroid populations were quantified, n=5 mice and 10 spheroids from each mice. Data are resented as means ± SEM, n=5, ***, P<0.001 (two-sided student's t-test).

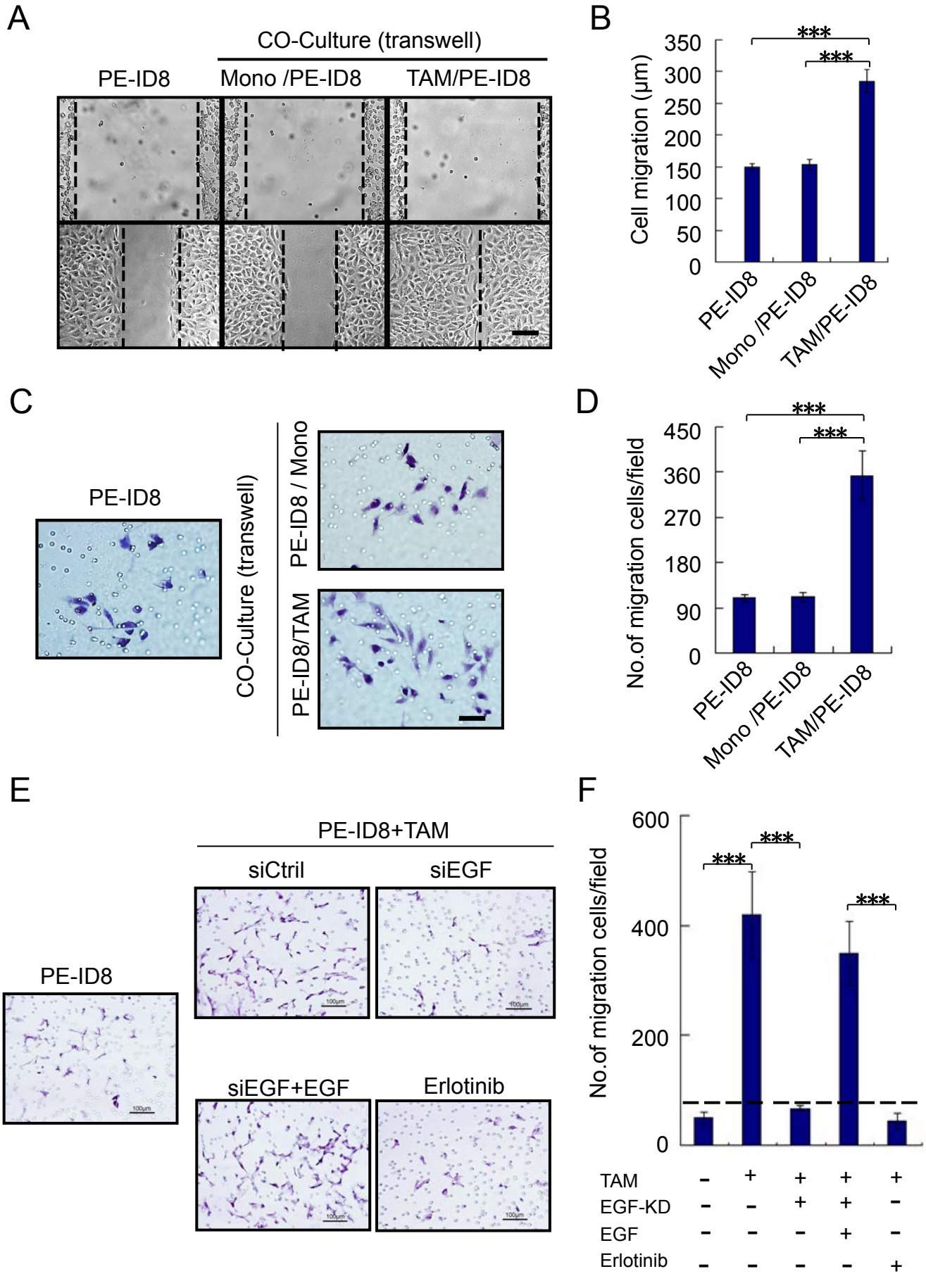
A
CO-Culture (transwell)
PE-ID8
Mono /PE-ID8
TAM/PE-ID8
B
Cell migration (μm)
350
300
250
200
150
100
50
0
***
***
PE-ID8
Mono /PE-ID8
TAM/PE-ID8
C
PE-ID8
CO-Culture (transwell)
PE-ID8 / Mono
PE-ID8/TAM
D
No.of migration cells/field
450
360
270
180
90
0
***
***
PE-ID8
Mono /PE-ID8
TAM/PE-ID8
E
PE-ID8+TAM
siCtril
siEGF
PE-ID8
siEGF+EGF
Erlotinib
F
No.of migration cells/field
600
400
200
0
***
***
***
TAM
EGF-KD
EGF
Erlotinib

Supplemental Figure 10. TAMs promote the migration of tumor cells through secreting EGF. (**A-B**) ID8 cells were cultured alone, or co-cultured with mouse monocytes or TAMs using a transwell. ID8 migration was analyzed by a wound-healing assay. Representative images and statistical analysis of tumor cell migration, n=3. Scale bar, 100μm. (**C-D**) ID8 cells were cultured alone, or co-cultured with mouse monocytes or TAMs using a transwell. ID8 migration was analyzed by counting cells migrated cross the transwell. Hematoxylin staining and statistical analysis of migrated tumor cells, n=3. Scale bar, 50μm. (**E-F**) TAMs were pre-transfected with control siRNA or EGF siRNAs for 48 h. ID8 cells were co-cultured with TAMs using a transwell in the absence or presence of EGF (20 ng/ml) or EGFR inhibitor erlotinib (20 μM) in the PE-ID8 culture media. Hematoxylin staining and statistical analysis of migrated tumor cells. Scale bar, 100μm. All data are presented as means ± SEM, n=3; ***, $P<0.001$ (two-sided student's t-test).

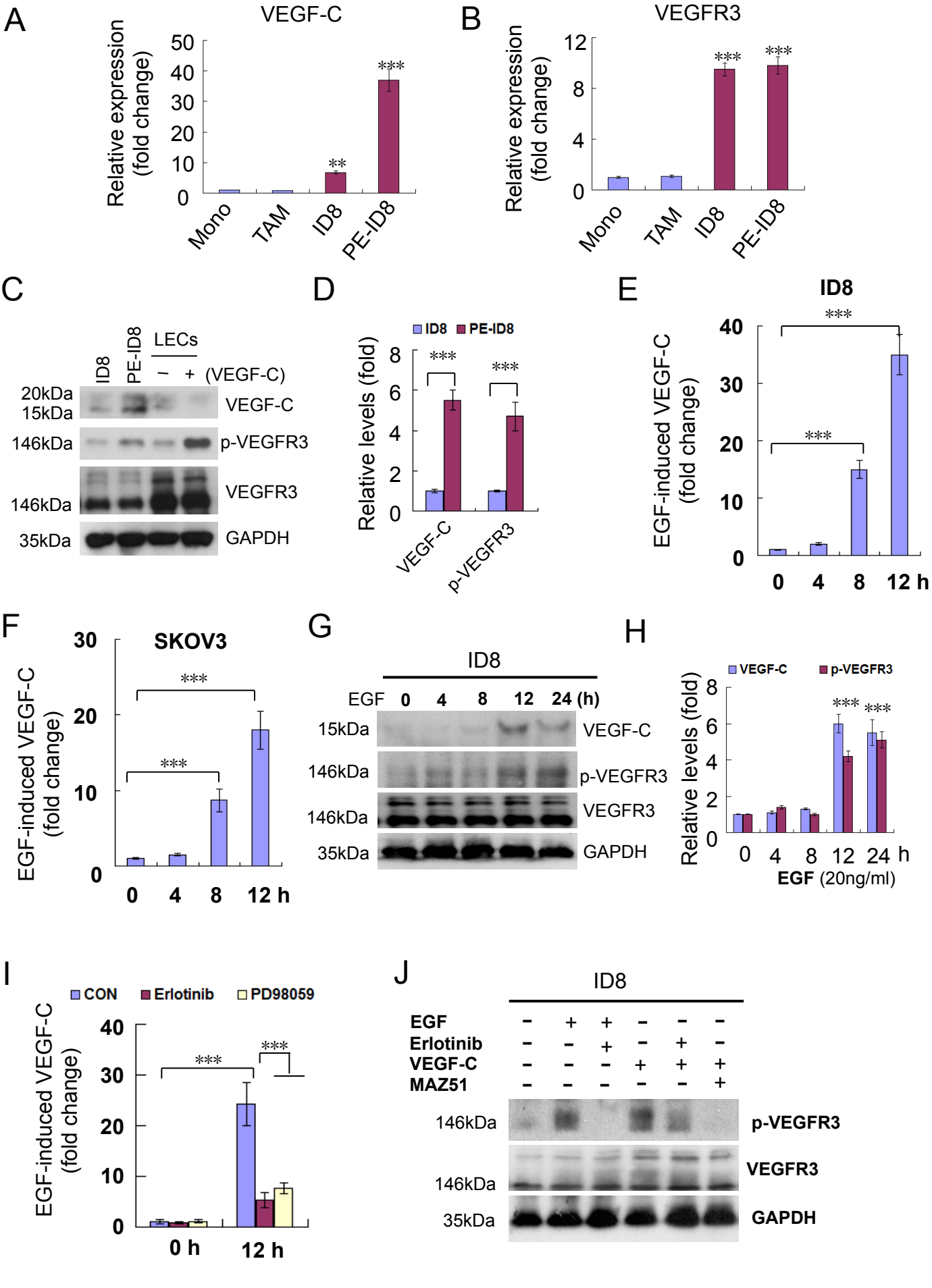
A
VEGF-C
Relative expression (fold change)
50
40
30
20
10
0
**
***
Mono
TAM
ID8
PE-ID8
B
VEGFR3
Relative expression (fold change)
12
8
4
0
***
***
Mono
TAM
ID8
PE-ID8
C
ID8
PE-ID8
LECs
–
+
(VEGF-C)
20kDa
15kDa
VEGF-C
146kDa
p-VEGFR3
146kDa
VEGFR3
35kDa
GAPDH
D
ID8
PE-ID8
Relative levels (fold)
8
6
4
2
0
***
***
VEGF-C
p-VEGFR3
E
ID8
EGF-induced VEGF-C (fold change)
40
30
20
10
0
***
***
0
4
8
12 h
F
SKOV3
EGF-induced VEGF-C (fold change)
30
20
10
0
***
***
0
4
8
12 h
G
ID8
EGF
0
4
8
12
24 (h)
15kDa
VEGF-C
146kDa
p-VEGFR3
146kDa
VEGFR3
35kDa
GAPDH
H
VEGF-C
p-VEGFR3
Relative levels (fold)
8
6
4
2
0
***
***
0
4
8
12
24 h
EGF (20ng/ml)
I
CON
Erlotinib
PD98059
EGF-induced VEGF-C (fold change)
40
30
20
10
0
***
***
0 h
12 h
J
ID8
EGF
Erlotinib
VEGF-C
MAZ51
146kDa
p-VEGFR3
146kDa
VEGFR3
35kDa
GAPDH

Supplemental Figure 11. EGF upregulates VEGF-C-VEGFR3 signaling in OC tumor cells. (**A-B**) Gene expression of VEGF-C and VEGFR3 in isolated TAMs and PE-ID8 tumor cells by qRT-PCR. Relative gene expressions are presented as fold changes by taking monocytes as 1.0, n=3. (**C**) VEGF-C, phosphorylations of VEGFR3 and total VEGFR3 were determined by Western blot with specific antibodies in ID8 and PE-ID8 cells. Lymphatic vascular endothelial cells (LECs) with or without VEGF-C (20 ng/ml) treatment were used as positive control. (**D**) Relative VEGF-C and phosphor-VEGFR3 levels were quantified. (**E,F**) Mouse ID8 and human SKOV3 OC cells were treated with EGF (20 ng/ml) for different times (0-12 h). VEGF-C mRNA was determined by qRT-PCR. Normalized VEGF-C mRNA levels (with GADPH) are presented as fold changes by taking untreated as 1.0. (**G-H**) ID8 cells were treated with EGF for different times. Total VEGF-C, phosphor- and total VEGFR3 were determined. Relative levels VEGF-C, phosphor-VEGFR3 were quantified. (**I**) SKOV3 cells were treated with EGF in the absence or presence of EGFR inhibitor (20 μM) or ERK inhibitor (PD98059; (20 μM) for 12 hrs. VEGF-C mRNA was determined by qRT-PCR. Normalized VEGF-C mRNA levels (with GADPH) are presented as fold changes by taking untreated as 1.0. (**J**) ID8 cells were treated with EGF in the absence or presence of EGFR inhibitor Erlotinib (20μM) for 12 h. Phosphor- and total VEGFR3 were determined. VEGF-C treatment (20 ng/ml for 5 min) was used as control. All data are presented as means ± SEM, n=3; ***, $P<0.001$ (two-sided student's *t*-test).

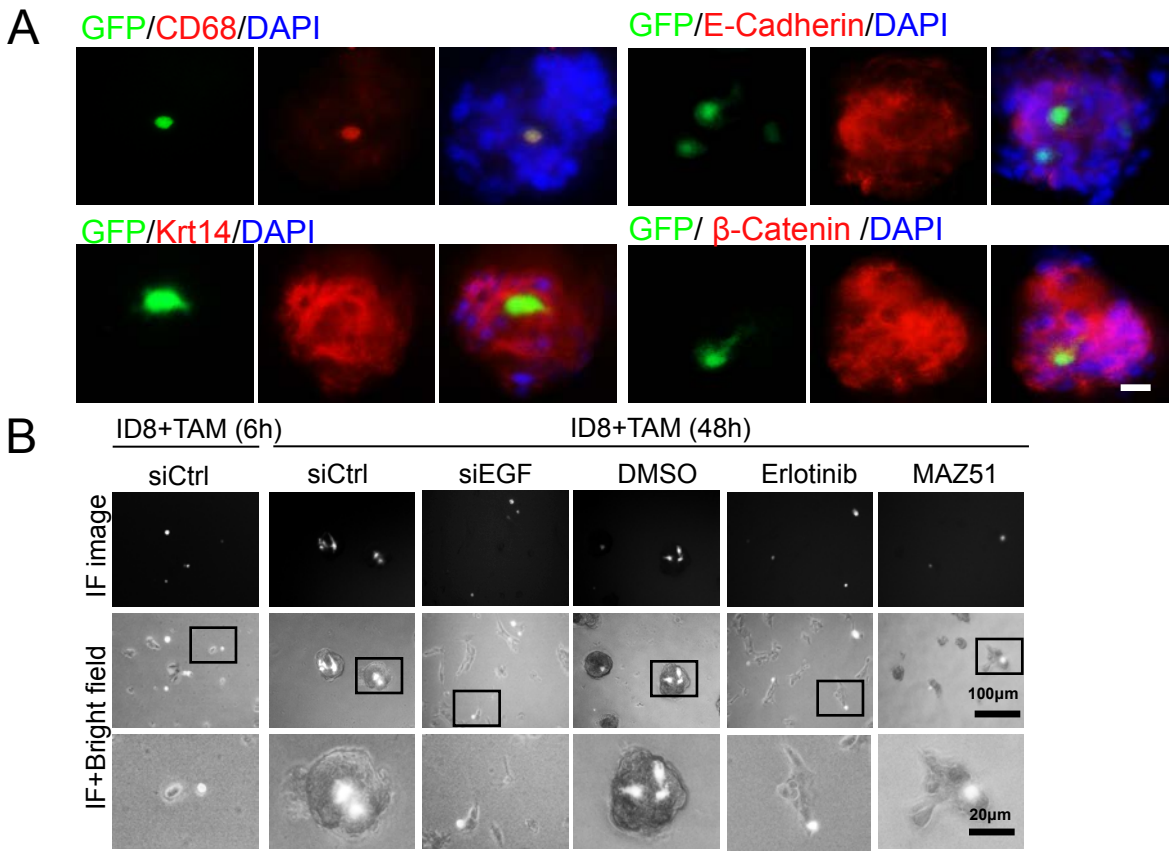

Supplemental Figure 12. Macrophage and tumor cell markers expression in spheroids in an in vitro 3D co-culture system. (**A**) $GFP^+F4/80^+CD206^+$ TAMs isolated from spheroids of ovarian cancer-bearing donor tomatolyzM-cre mice. Immunofluorescent co-stainings of GPF with CD68, E-Cadherin, Keratin 14 or β-Catenin in spheroids. Scale bar, 10 μm.

(**B**) TAMs were pre-transfected with Ctrl-siRNA or EGF-siRNA for 48 h. ID8 cells were co-cultured with modified TAMs in a 3D co-culture system. TAMs were mixed with ID8 cells (TAMs:ID8 ratio as 1:10), a total of 40,000 cells in medium containing 2% matirgel were seeded onto the 24-well precoated with matrigel. Erlotinib or MAZ51 (20

) was added to tumor cells at 6 h after co-culture. Representative picture show GFP^+ cells (TAMs) localization in the center of spheroid (B: black/white). (Scale bar, 20 or 100μm).

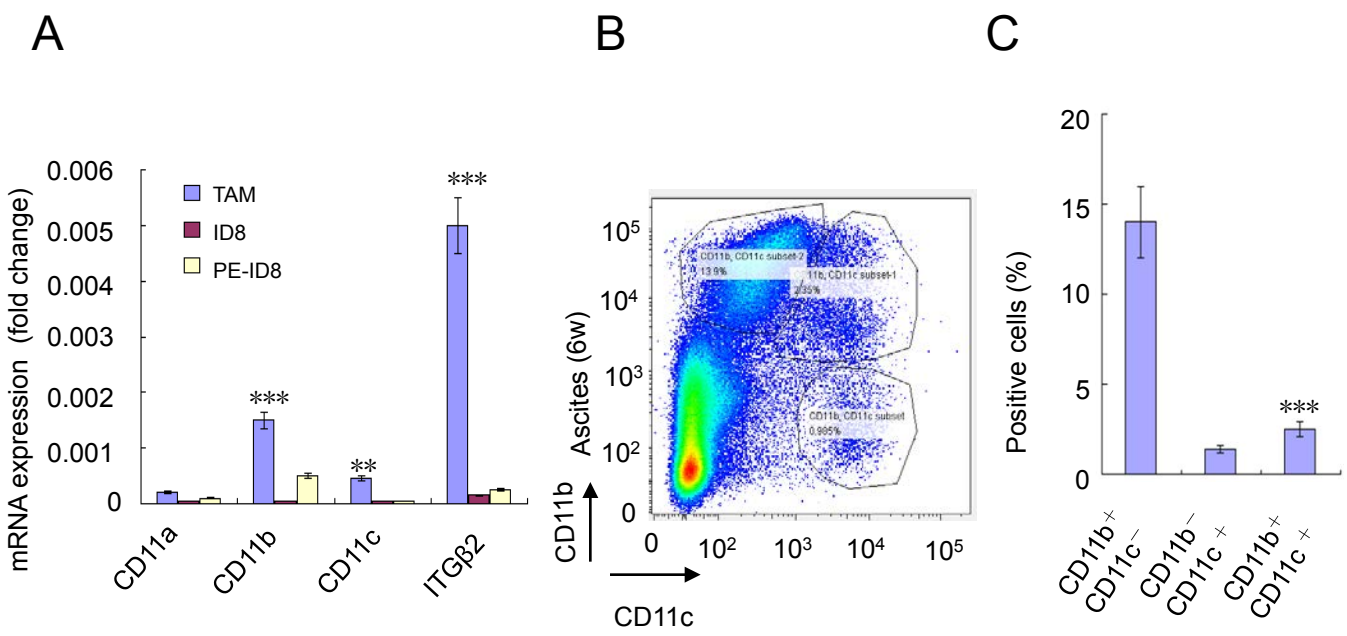

Supplemental Figure 13. CD11b, CD11c and β2 expression in TAMs. TAMs and PE-ID8 in the orthotopic ovarian cancer model were harvested from spheroids at indicated times (8 weeks). (**A**) CD11a, CD11b, CD11c and β2 integrin in TAMs and PE-ID8 were determined by qRT-PCR. Naïve ID8 cells were used as a control. All data are presented as means ± SEM, n=5, **, *P*<0.01; ***, *P*<0.001 (two-sided student's *t*-test). (**B-C**) $CD11b^+$ and $CD11c^+$ macrophages in peritoneal cavity were analyzed by FACS (**B**). % of CD11b+ cells and % of $CD11c^+$ cells were quantified (**C**), n=5, ***, *P*<0.001; ns: non-significance. (two-sided student's t-test). Three independent experiments were performed. Data are presented as means ± SEM, **, P<0.01; ***, *P*<0.001.

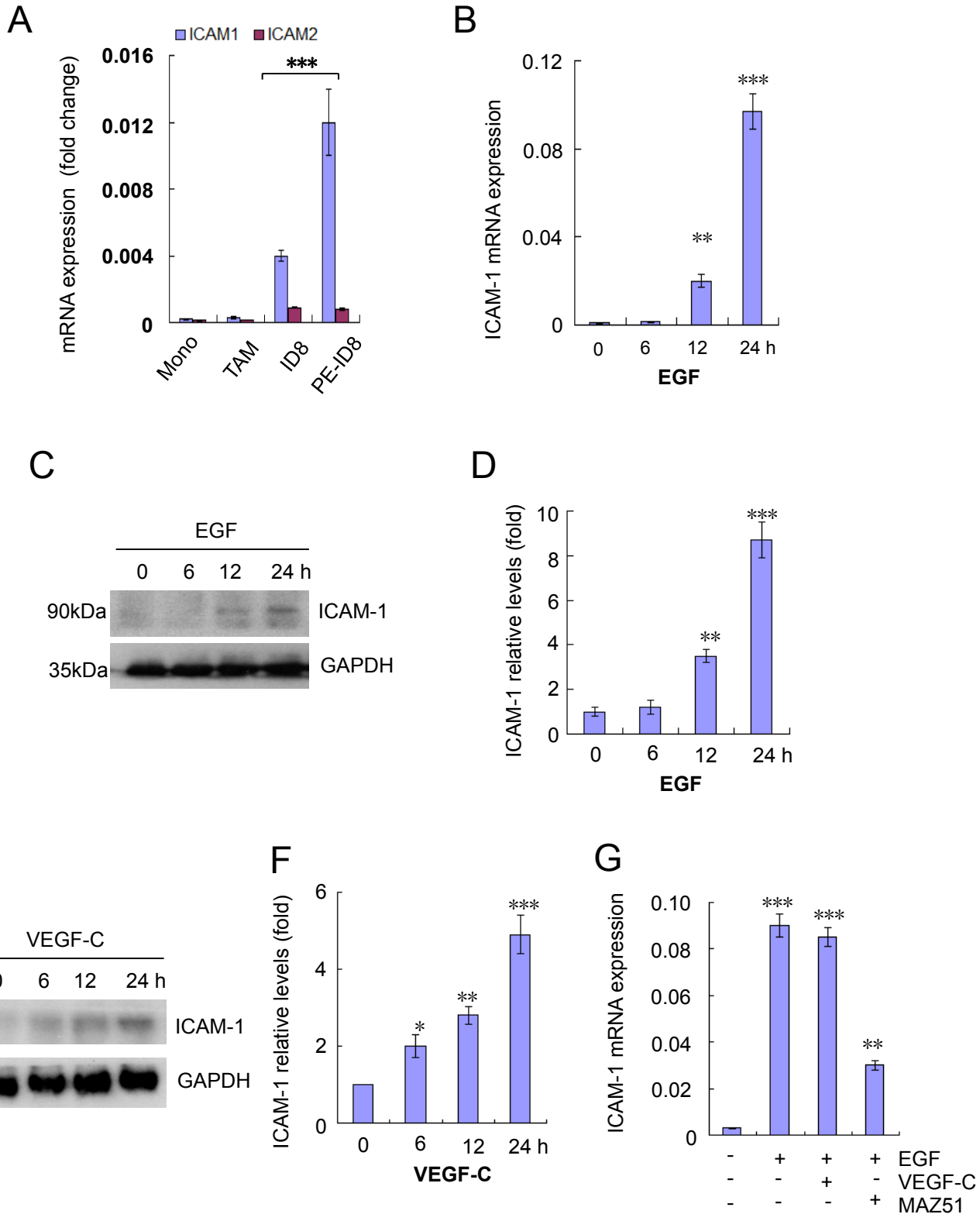
A
ICAM1
ICAM2
mRNA expression (fold change)
0.016
0.012
0.008
0.004
0
***
Mono
TAM
ID8
PE-ID8
B
ICAM-1 mRNA expression
0.12
0.08
0.04
0
**
***
0
6
12
24 h
EGF
C
EGF
0
6
12
24 h
90kDa
ICAM-1
35kDa
GAPDH
D
ICAM-1 relative levels (fold)
10
8
6
4
2
0
**
***
0
6
12
24 h
EGF
E
VEGF-C
0
6
12
24 h
90kDa
ICAM-1
35kDa
GAPDH
F
ICAM-1 relative levels (fold)
6
4
2
0
*
**
***
0
6
12
24 h
VEGF-C
G
ICAM-1 mRNA expression
0.10
0.08
0.06
0.04
0.02
0
***
***
**
- + + + EGF
- - + - VEGF-C
- - - + MAZ51

Supplemental Figure 14. The EGF/EGFR-VEGF-C/VEGFR3 signaling pathway induces ICAM-1 expression in spheroids. TAMs and PE-ID8 in the orthotopic ovarian cancer model were harvested from spheroids at indicated times (8 weeks). (**A**) ICAM-1 and ICAM-2 were determined by qRT-PCR. Peripheral blood monocytes were used as a control. All data are presented as means ± SEM, n=5, **, $P<0.01$ (two-sided student's *t*-test). (**B**) ID8 cells were treated with EGF for different times. ICAM-1 was determined by qRT-PCR and relative levels ICAM-1 was quantified. Three independent experiments were performed. Data are presented as means ± SEM, **, $P<0.01$; ***, $P<0.001$ (two-sided student's *t*-test). (**C-F**) ID8 cells were treated with EGF (**C**) or VEGF-C (**E**) for different times. ICAM-1 was determined by Western blot with specific antibodies. (**D, F**) Relative protein levels were quantified. Three independent experiments were performed. Data are presented as means ± SEM, n=3, ***, $P<0.001$ (two-sided student's *t*-test). (**G**) ID8 cells were treated with EGF or VEGF-C in the absence or presence of VEGFR3 inhibitor (MAZ51) for 24 hours. ICAM-1 was determined by qRT-PCR and relative levels ICAM1 was quantified. Three independent experiments were performed. Data are presented as means ± SEM, **, $P<0.01$; ***, $P<0.001$ (two-sided student's *t*-test).

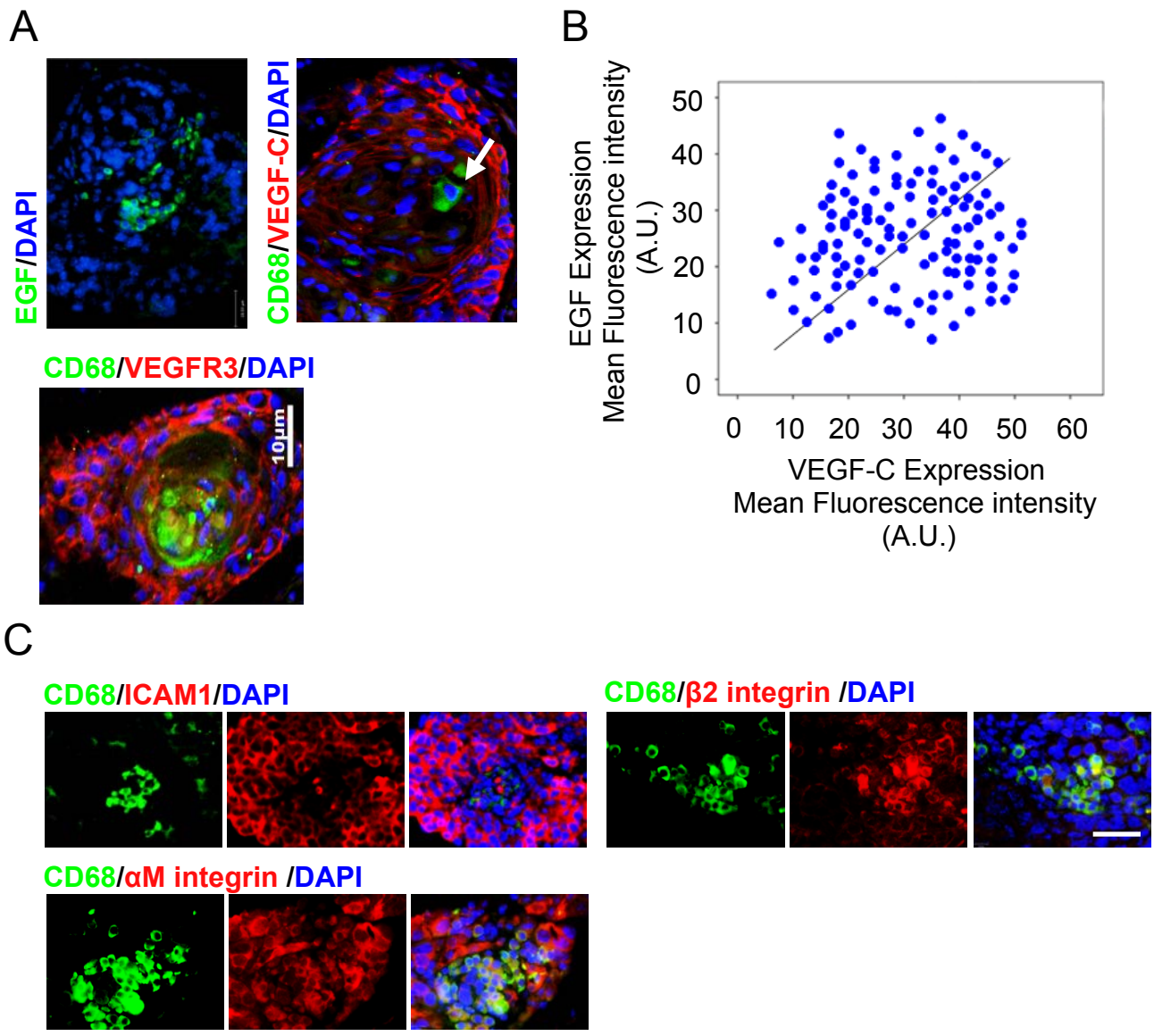

Supplemental Figure 15. Expression of VEGF-C, VEGFR3, ICAM-1, αM integrin and β2 integrin in TAMs and tumor cells of OC patients. (**A**) Immunofluorescent stainings of spheroids harvested from ascites of OC patients. Co-stainings of EGF and CD68 with VEGF-C or VEGFR3. Representative images of spheroids from n=128 OC patients are shown. $CD68^+$ TAMs in the center of spheroids are indicated by arrows. Scale bar, 10 µm. (**B**) Relative mean fluorescence intensity calculated using Image J for cell clusters from 128 OC patients. Statistical significance at (R=0.715, p=0.002). (**C**) Immunofluorescent co-stainings of CD68 with ICAM-1, αM integrin or β2 integrin in spheroids harvested from ascites of OC patients. Representative images of spheroids from n=128 OC patients are shown. Scale bar, 20 µm, (two-sided student's t-test).

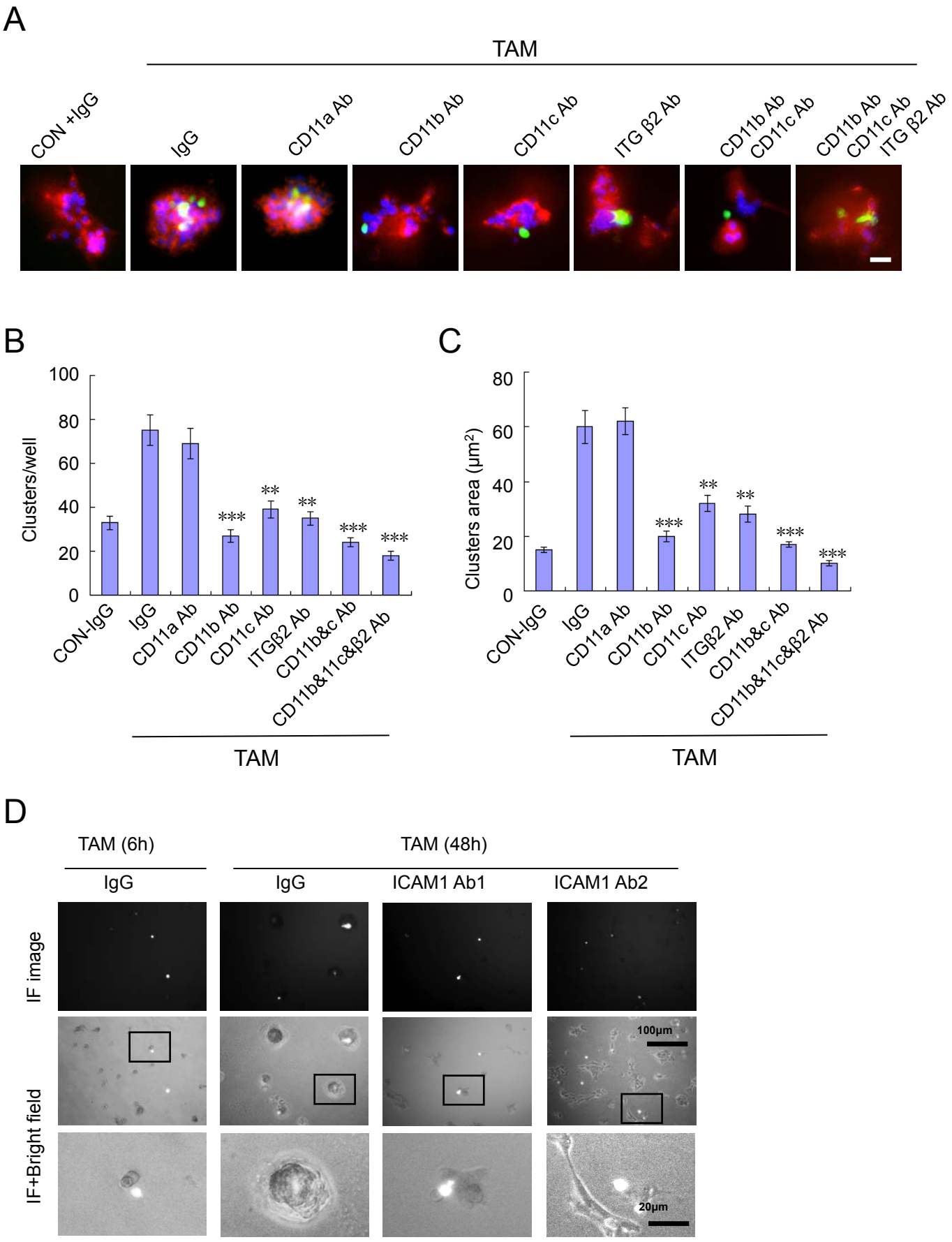
A
TAM
CON +IgG
IgG
CD11a Ab
CD11b Ab
CD11c Ab
ITG β2 Ab
CD11b Ab CD11c Ab
CD11b Ab CD11c Ab ITG β2 Ab
B
Clusters/well
100
80
60
40
20
0
**
***
CON-IgG
IgG
CD11a Ab
CD11b Ab
CD11c Ab
ITGβ2 Ab
CD11b&c Ab
CD11b&11c&β2 Ab
TAM
C
Clusters area (μm²)
80
60
40
20
0
D
TAM (6h)
TAM (48h)
IgG
ICAM1 Ab1
ICAM1 Ab2
IF image
IF+Bright field
100μm
20μm

Supplemental Figure 16. integrins CD11b, CD11c, β2 and adhesion molecule ICAM-1 play important role in spheroid formation. (A-C). 3D co-cultures of mouse ID8 cells without TAM (CON) or with TAMs (+TAM). Control IgG or neutralizing antibodies to CD11a, CD11b, CD11c or β2 integrin (20 μg/ml each). Number and size of spheroids were measured at 48 h. Representative images are in (**A)**. Scale bar, 50 μm. Quantifications of spheroid number and size in (**B-C)**. (**D**) Isotype IgG or an anti-mouse ICAM-1 antibody (20 μg/ml each) was added to 3D co-culture. Number and size of spheroids were measured periodically at 6 h and 48 h. Representative pictures show GFP^+ cells (TAMs) localization in spheroid. Scale bar, 20 μm (middle panel) or 100 μm (bottom panel).
Three independent experiments were performed. Data are presented as means ± SEM, **, P<0.01; ***, *P*<0.001.

Supplemental Table 1, related to Supplemental Figure 7

Demographic characteristics of patients with epithelial ovarian cancer

Characteristics	CD68-positive cells in Spheroids (%)	No. of patients(N=128)	*P*
Age (years)			0.450
<50	14.3±0.5	45	
≥50	14.8±0.4	83	
Lymph node metastasis			0.013
Absent	13.2±0.4	88	
Present	16.7±0.7	40	
Histopathological differentiation			<0.0001
Well	10.3±0.5	27	
Moderate	13.8±0.2	41	
Poor	19.8±0.9	60	
Histology type			0.134
Serous adenocarcinoma	14.8±0.4	95	
Mucoid adenocarcinoma	14.3±0.8	15	
Endometrioid adenocarcinoma	14.2±0.3	18	
Chemotherapy regimen			0.21
TP	14.7±0.2	60	
PAC	14.3±0.9	68	
Ascites			0.009
＜100	11.7±0.2	38	
⩾100	16.7±0.9	90	
Primary tumor size (cm)			
＜5	14.2±0.2	55	0.19
⩾5	14.7±0.9	73	
Serum CA-125 level (U/ml)			
＜35	12.1±0.2	17	0.0043
⩾35	15.7±0.9	111	

TP: cisplatin and paclitaxel; PAC: cisplatin, epirubicin and cyclophosphamide.

Supplemental Table 2, related to Supplemental Figure 7

Univariate analysis of 128 patients with epithelial ovarian cancer

Variables	OS		*P*
	5-year (%)	χ^2	
CD68 expression		18.630	<.0001
<14.5	61.4		
≥ 14.5	22.5		
Lymph node metastasis		11.876	0.0006
Absent	51.4		
Present	17.5		
Histopathological differentiation		9.926	0.001
Well	46.3		
Moderate	39.2		
Poor	26.7		
Histology type		1.5304	0.465
Serous adenocarcinoma	36.9		
Mucoid adenocarcinoma	53.3		
Endometrioid adenocarcinoma	36.8		
Age (years)		0.287	0.592
<50	40.0		
≥ 50	39.8		
Chemotherapy regimen		41.912	<.0001
TP	61.45		
PAC	16.36		
Ascites		7.235	0.008
＜100	0.668		
⩾100	0.4583		
Primary tumor size (cm)		3.451	0.011
＜5	0.556		
⩾5	0.498		
Serum CA-125 level (U/ml)		9.43	0.0015
＜35	0.7333		
⩾35	0.4554		

OS: overall survival time; TP: cisplatin and paclitaxel; PAC: cisplatin, epirubicin and cyclophosphamide.

Supplemental Table 3, related to Supplemental Figure 7

Multivariate analysis with covariates adjustment of 128 patients with epithelial ovarian cancer

Variables	OS [a]		*P*
	HR	*95%CI*	
CD68 expression	2.590	1.073, 6.250	0.034
<14.5			
≥ 14.5			
Lymph node metastasis	1.734	1.031, 2.918	0.038
Absent			
Present			
Histopathological differentiation	0.668	0.277, 1.607	0.368
Well	0.585	0.197,1.735	0.333
Moderate			
Poor			
Chemotherapy regimen [b]	3.031	1.809, 6.026	0.0001
TP			
PAC			
Age (years)	1.110	0.672, 1.834	0.683
<50			
≥ 50			

[a]: Likelihood Ratio test, *P*<.0001; OS: overall survival time; [b]TP: cisplatin and paclitaxel; PAC: cisplatin, epirubicin and cyclophosphamide.

Supplemental Experimental Procedures

Counting tumor (mCherry) and macrophage (GFP^+) in ascites

ID8 OC cells stably expressing mCherry fluorescence protein were implanted into 8-weeks old $tomato^{lyz\text{-}cre}$ recipient mice. $Cherry^+$ tumor cells and GFP^+ cells infiltrated into peritoneal cavity were detected at indicated times post-tumor cell implantation, and five mice were harvested at every time point. Collected ascites and counting total number by fluorescence microscope.

Monoclonal antibodies

Two blocking anti-mouse ICAM1 (cd54) and one blocking anti-human ICAM1 antibodies were used in these studies. Rat anti-mouse ICAM-1 monoclonal antibody YN1/1 was purified as previously described (1,2). Rat IgG was used as a control antibody (Santa cruz, Cat:sc-2026). Azide-free hamster anti-mouse ICAM1 monoclonal antibody 3E2 was purchased from BD Pharmingen (San Diego, CA). Anti-human ICAM1/CD54 antibody was purchased from R&D systems Inc (Minneapolis, MN; Cat: BBA3) Nonimmune hamster IgG was purchased from Pierce (Rockford, IL). These three antibody has also been shown to inhibit the function of murine ICAM1 (3-6).

3D co-culture system of TAM and ID8 cells

Mouse $F4/80^+CD206^+$TAMs were isolated by FACS sorting from spheroids of ovarian cancer-bearing donor $tomato^{lyzM\text{-}cre}$ mice. Human tumor spheroids from advanced stage (ie, Stage III-IV) ovarian cancer patients were harvested (IHC protocol # 1111003959) followed by FACS sorting for CD14+ TAMs. The 24-well plates were precoated with matrigel as described above. The mixtures of TAMs and ID8 cells (at ratio of 1:10 but with a fixed total cell number as 40,000 cells / well) were directly seeded onto the matrigel-precoated 24 well plate. The cells were incubated at 37℃ for up to 48 hours to allow the aggregates/spheroids to form. EGFR inhibitor Erlotinib, VEGFR3 inhibitor MAZ51 (20 nM each), CD11a (10 μg/ml), CD11b (10 μg/ml), CD11c (10 μg/ml), Integrin β2 (10 μg/ml) or anti-ICAM-1 antibody (20 μg/ml) was added at 6 h after co-culture. Fluorescent microscopic images were taken to analyze the morphology from 6 – 48 h. The wells without cells but containing medium were used as negative control. All assays were performed at least three times and each time was tested in triplicate. All microscopical images were observed using Zeiss Axiovert 200 fluorescence microscope (Carl Zeiss MicroImaging; Thornwood, NY), and images were captured using Openlab3

software (Improvision, Lexington, MA) (7,8).

In vivo treatment in mouse models

Mice were divided into groups of ten mice per group. An orthotopic mouse model was established by injecting mouse ID8 OCs intraperitoneally to C57BL/6 female recipient mice. For LC treatment, LC was administrated subcutaneously (s.c) at 10 μl/g body weight every four days (except 20 μl/g at the first dose). For EGFR inhibitor treatment, Erlotinib was injected intraperitoneally (i.p) at 100 mg/kg body weight/ Day. For antibody treatment, mice were injected i.p. with normal rat IgG or rat anti-ICAM1 antibody (5 mg/kg, 1 time/3 days). Experimental and control mice were killed at 50 days after injected tumor cells. Collected ascites and spheroid for H&E staining and FACS.

Patients and tissue samples

Following Institutional Review Board approval, a total of 128 patients with advanced epithelial ovarian cancer (EOC) from the research files at The Tumor Hospital of Harbin Medical University who were seen from Jan. 2005 to Dec. 2009, and who met our inclusion criteria, were entered in this study. The eligibility criteria included the following: (1) pathologic examination confirming the presence of stage III EOC; (2) complete basic clinical data; (3) absence of any prior treatment for cancer; (4) no serious complications or other malignant disease; (5) the patients and family members being informed about the illness and having given informed consent before treatment. All patients had undergone complete cytoreductive surgery.

Immunohistochemical Staining

Paraffin-embedded spheroid samples isolated from the ascites of EOC patients (128 cases) were sectioned at a thickness of 4μm. To stain CD68, the slides were first deparaffinized in xylene and rehydrated with gradient concentrations of alcohol under standard procedures. After rehydration, the slides were immersed in 0.01 mol/L citrate buffer (pH 6.0) and heated (95°C) for 15 min for antigen retrieval. Then, the samples were incubated with 3% hydrogen peroxide (H_2O_2) for 10 minutes followed by 10% normal goat serum blocking for 10 minutes. Subsequently, the sections were incubated with primary rabbit polyclonal anti-human CD68 antibody (dilution 1:100) (sc-20060, Santa Cruz Biotechnology) for 1 hour at room temperature. After washing with PBST for 3 times, the

sections were incubated with biotin-labeled secondary antibody followed by horseradish peroxidase (HRP)-conjugated streptavidin for 30 minutes individually at room temperature. After applying HRP substrate, 3.3'-diaminobenzidine tetrahydrochloride (D3939-1set, Sigma) in 0.01% H_2O_2, for 10 minutes, the slides were counterstained with Meyer's hematoxylin for 30 to 60 seconds and mounted with mounting medium for visualization under microscope (9,10).

Semi-Quantitative Analysis of CD68 Staining

Scoring of CD68 in EOC samples via IHC staining follows the methods previously published. All of IHC staining samples from EOC patients were evaluated by experienced two pathologists independently.

Quantitative Analysis of EGF and VEGF-C Staining

Quantitative comparison of EGF and VEGF-C expression was determined using the freeware image analysis software, Image J, WS Rasband, National Health Institute, Bethesda, MA, USA) as previously reported (11). Cell area was determined by manual delineation of raw fluorescence images. A minimum of 12 cells were analyzed from two independent experiments.

Follow-up evaluation

During the follow-up period, EOC patients with post-cytoreductive surgery and chemotherapy were requested to perform serum CA-125 test, pelvic MRI, color Doppler ultrasound of the liver and kidney, and pulmonary X-rays every three months in the first two years, every six months from 3 to 5 years, and annually thereafter. The end points of the study were progression-free (PFS) and overall survival (OS) as reported (12).

Supplemental Table 5

Primes for qPCR (human and mouse)

Primer	Forward Sequence	Reverse Sequence
Mouse		
ARG1	CTCCAAGCCAAAGTCCTTAGAG	AGGAGCTGTCATTAGGGACATC
CCL2	TTAAAAACCTGGATCGGAACCAA	GCATTAGCTTCAGATTTACGGGT
CCR2	ATCCACGGCATACTATCAACATC	CAAGGCTCACCATCATCGTAG
CD3e	GAGAGAGAATTCTGAGAGGATGCGG	GTCAGACTGCTCTCTGATTCAGGCC
CD11a	CCAGACTTTTGCTACTGGGAC	GCTTGTTCGGCAGTGATAGAG
CD11b	GGCTCCGGTAGCATCAACAA	ATCTTGGGCTAGGGTTTCTCT
CD11c	CTGGATAGCCTTTCTTCTGCTG	GCACACTGTGTCCGAACTCA
CD68	TGTCTGATCTTGCTAGGACCG	GAGAGTAACGGCCTTTTTGTGA
CD163	GGTGGACACAGAATGGTTCTTC	CCAGGAGCGTTAGTGACAGC
CD206	CTCTGTTCAGCTATTGGACGC	TGGCACTCCCAAACATAATTTGA
CX3CR1	ACGAAATGCGAAATCATGTGC	CTGTGTCGTCTCCAGGACAA
CXCR4	CTTCTGGGCAGTTGATGCCAT	CTGTTGGTGGCGTGGACAAT
EGF	AGCATCTCTCGGATTGACCCA	CCTGTCCCGTTAAGGAAAACTCT
EGFR	GCCATCTGGGCCAAAGATACC	GTCTTCGCATGAATAGGCCAAT
FGF2	GCGACCCACACGTCAAACTA	CCGTCCATCTTCCTTCATAGC
FGFR	GCTATAAGGTACGAAACCAGCAC	GGTTGATGGACCCGTATTCATTC
HGF	ACTTCTGCCGGTCCTGTTG	CCCCTGTTCCTGATACACCT
ICAM1	GTGATGCTCAGGTATCCATCCA	CACAGTTCTCAAAGCACAGCG
ICAM2	TGGTCCGAGAAGCAGATAGTAG	GAGGCTGGTACACCCTGATG
IL10	AGAAGCATGGCCCAGAAATCA	GGCCTTGTAGACACCTTGGT
INFαR	CTTCCACAGGATCACTGTGTACCT	TTCTGCTCTGACCACCTCCC
iNOS	ACATCGACCCGTCCACAGTAT	CAGAGGGGTAGGCTTGTCTC
ITGB2	CAGGAATGCACCAAGTACAAAGT	CCTGGTCCAGTGAAGTTCAGC
Ly6G/C	GACTTCCTGCAACACAACTACC	ACAGCATTACCAGTGATCTCAGT
PDGFA	ACCTCCAGCGACTCTTGG	TTCTCGGGCACATGGTTA
PDGFAR	AGACCTGGACATCTTTGG	TGTAGTCGCCGTTATTTT
PDGFB	GGTCAAACCTCTGAGGAAAGG	AGTACCATGGGCTCATTCTGA
PDGFBR	CCAGAAGTAGCGAGAAGC	ATCACCGTATCGGCAGTA
PIGF	TCCTTCTTCGTGGACAACTTCT	GTACGACAAGAGATTGACAGTGG
SDF1	GTCAGCCTGAGCTACCGATG	TTCTTCAGCCGTGCAACAATC
TNF-α	CCCTCACACTCAGATCATCTTCT	GCTACGACGTGGGCTACAG
TGF-β	AGCACAGTATGCAAGCCTCG	ATCTGTAATGTTGAACTGGGTGG
VEGFC	TGCCGATGCATGTCTAAACT	TGAACAGGTCTCTTCATCCAGC
VEGFR3	ACAGAAGCTAGGCCCTACTG	ACCCACATCGAGTCCTTCCT
Human		
CD68	GGAAATGCCACGGTTCATCCA	TGGGGTTCAGTACAGAGATGC
EGF	TGGATGTGCTTGATAAGCGG	ACCATGTCCTTTCCAGTGTGT
EGFR	CCCACTCATGCTCTACAACCC	TCGCACTTCTTACACTTGCGG

ICAM1	ATGCCCAGACATCTGTGTCC	GGGGTCTCTATGCCCAACAA
ITGAM	GCCTTGACCTTATGTCATGGG	CCTGTGCTGTAGTCGCACT
ITGB2	TGCGTCCTCTCTCAGGAGTG	GGTCCATGATGTCGTCAGCC
VEGFC	GAGGAGCAGTTACGGTCTGTG	TCCTTTCCTTAGCTGACACTTGT
VEGFR3	TGCACGAGGTACATGCCAAC	GCTGCTCAAAGTCTCTCACGAA

Supplemental Table 4

List of antibodies

Antibody name	Company	Host Species	Cat No.	Usage	Dilution
α M integrin	BD Pharmingen	Rat	557395	WB	1:500
β 2 integrin	Santa Cruz	Mouse	SC-8420	WB	1:500
β-Actin	Gene Tex Inc	Rabbit	GTX109639	WB	1:2000
β-Catenin	BD Pharmingen	Mouse	51-9001922	IF	1:200
AKT1/2/3	Santa Cruz	Rabbit	sc-8312	WB	1:1500
p-AKT1	Cell signaling	Rabbit	#4060	WB	1:1000
CCL2(R-17)	Santa Cruz	Goat	sc-1785	IF	1:50
CCR2	abcam	Rabbit	ab21667	IF	1:100
CD11a(M17/4)	Biolegend	Rat	101110	Function	10 μ g/ml
CD11b	BD Pharmingen	Rat	557395	IF	1:100
CD11b(1/70)	Biolegend	Rat	101214	Function	10 μ g/ml
CD11c (N418)	Biolegend	Hamster	117302	Function	10 μ g/ml
CD68	abcam	Mouse	ab31630	IF	1:100
CD68(KP1)	Santa Cruz	Mouse	sc-20060	IHC	1:50
CX3CR1	abcam	Rabbit	ab8021	IF	1:100
E-Cadherin	BD Pharmingen	Mouse	51-9001921	IF	1:200
EGF	abcam	Rabbit	ab9695	IF, WB	1:50,1:500
EGFR(1005)	Santa Cruz	Rabbit	sc-03	IF	1:100
EGFR	Cell signaling	Rabbit	#2232	IF, WB	1:100,1:1000
p-EGFR	Cell signaling	Rabbit	#2234	WB	1:500
ERK	Santa Cruz	Rabbit	sc-94	WB	1:1000
p-ERK	Cell signaling	Mouse	#9106	WB	1:1000
GAPDH	Cell signaling	Rabbit	#2118	WB	1:2000
ICAM1	Biolegend	Rat	116101	WB, Function	1:500 20 μ g/ml
ICAM1	BD Pharmingen	Mouse	550287	Function	50 μ g/ml
ICAM1	R&D systems Inc	Mouse	BBA3	Function	20 μ g/ml
Integrin β 2	Biolegend	Hamster	103507	Function	10 μ g/ml
Ki67	Cell signaling	Rabbit	#9129	IF	1:100
P38	Santa Cruz	Rabbit	sc-535	WB	1:1000
p-P38	Cell signaling	Rabbit	#4511	WB	1:1000
PI3K	Santa Cruz	Mouse	sc-1637	WB	1:500
p-PI3K	Cell signaling	Rabbit	#4228	WB	1:500
VEGFR3	R&D Systems	Mouse	AF743	IF	1:50
VEGF-C	abcam	Rabbit	ab9546	IF, WB	1:50,1:500
VEGFR3	Cell application	Rabbit	cb5792	WB	1:1000
p-VEGFR3	Cell application	Rabbit	cb5793	WB	1:500
FACS					
FITC-CD11b	Biolegend	Rat	101205	FACS	1:200
PE-F4/80	Biolegend	Rat	123109	FACS	1:200

APC-F4/80	Biolegend	Rat	100311	FACS	1:200
PE-CD206	Biolegend	Rat	141705	FACS	1:200
APC-CD163	Biolegend	Rat	333609	FACS	1:200
FITC-CD14	BD Biosciences	Mouse	347497	FACS	1:100

Supplemental References

1. Takei, F.(1985). Inhibition of mixed lymphocyte response by a rat monoclonal antibody to a novel murine lymphocyte activation antigen (MALA-2). J. Immunol. *134*:1403–1407.
2. Horley, K.J., C. Carpenito, B. Baker, and F. Takei. (1989). Molecular cloning of murine intercellular adhesion molecule (ICAM-1). EMBO (Eur. Mol. Biol. Organ.) J. *8*:2889–2896.
3. Schynius, A., R.L. Camp, and E. Pure. (1993). Reduced contact sensitivity reactions in mice treated with monoclonal antibodies to leukocyte functionassociated molecule-1 and intercellular adhesion molecule-1. J. Immunol. *150*: 655–663.
4. Kumasaka T, Quinlan WM, Doyle NA, Condon TP, Sligh J, Takei F, Beaudet Al, Bennett CF, Doerschuk CM. (1996). Role of the intercellular adhesion molecule-1(ICAM-1) in endotoxin-induced pneumonia evaluated using ICAM-1 antisense oligonucleotides, anti-ICAM-1 monoclonal antibodies, and ICAM-1 mutant mice. J Clin Invest. 1996;*97(10)*:2362-9.
5. Prieto, J., F. Takei, R. Gendelman, B. Christenson, P. Biberfeld, and M. Patarroyo. (1989). MALA-2, mouse homologue of human adhesion molecule ICAM-1 (CD54). Eul: J. Imrnunol. 19:1551.
6. Suárez Y, Wang C, Manes TD, Pober JS. Cutting edge: TNF-induced microRNAs regulate TNF-induced expression of E-selectin and intercellularadhesion molecule-1 on human endothelial cells: feedback control of inflammation. J Immunol. 2011;186(3):1763-8.
7. Hagemann T, Wilson J, Burke F, Kulbe H, Li NF, Plüddemann A, Charles K, Gordon S, Balkwill FR. (2006). Ovarian cancer cells polarize macrophages toward a tumor-associated phenotype. J Immunol. *176(8)*: 5023-32.
8. Waffarn EE, Hastey CJ, Dixit N, Soo Choi Y, Cherry S, Kalinke U, Simon SI, Baumgarth N. Infection-induced type I interferons activate CD11b on B-1 cells for subsequent lymph node accu mulation. Nat Commun. 2015;6:8991.
9. Yin M., Li C., Li X., Lou G., Miao B., Liu X., Meng F., Zhang H., Chen X., Sun M., Ling Q., Zhou R. (2011). Over-expression of LAPTM4B is associated with poor prognosis and chemotherapy

resistance in stages III and IV epithelial ovarian cancer. Journal of surgical oncology *104*, 29-36.

10. Yin M., Xu Y., Lou G., Hou Y., Meng F., Zhang H., Li C., Zhou R. (2011) LAPTM4B overexpression is a novel predictor of epithelial ovarian carcinoma metastasis. Int J Cancer 129, 629-635.
11. Burgess, A.; Vigneron, S.; Brioudes, E.; Labbé, J.-C.; Lorca, T.; Castro, A. (2010) Loss of human Greatwall results in G2 arrest and multiple mitotic defects due to deregulation of the cyclin B-Cdc2/PP2A balance. Proc. Natl. Acad. Sci. USA, 107, 12564–12569.
12. Omura GA., Brady MF., Homesley HD., Yordan E., Major FJ., Buchsbaum HJ., Park RC. (1991) Long-term follow-up and prognostic factor analysis in advanced ovarian carcinoma: the Gynecologic Oncology Group experience. J Clin Oncol *9,* 1138-50.